Optical genome mapping reveals complex cytogenetic abnormalities in multiple myeloma

by Jorge A. Palacios, Mónica Bernal, Jose R. Vilchez, Pilar Garrido, Pilar JimØnez, Juan F. GutiØrrez-Bautista, María C. Barrera-Aguilera, Lucía Ballesta, Teresa Rodríguez, Maria J. Olivares-DurÆn and Francisco Ruiz-Cabello

Received: April 15, 2025.
Accepted: June 12, 2025.

Citation: Jorge A. Palacios, Mónica Bernal, Jose R. Vilchez, Pilar Garrido, Pilar JimØnez, Juan F. GutiØrrez-Bautista, María C. Barrera-Aguilera, Lucía Ballesta, Teresa Rodríguez, Maria J. Olivares-DurÆn and Francisco Ruiz-Cabello. Optical genome mapping reveals complex cytogenetic abnormalities in multiple myeloma.
Haematologica. 2025 June 19. doi: 10.3324/haematol.2025.288008 [Epub ahead of print]

Optical genome mapping reveals complex cytogenetic abnormalities in multiple myeloma

Jorge A. Palacios[1,2], Mónica Bernal[2,3], Jose R. Vílchez[2,3], Pilar Garrido[1,2], Pilar Jiménez[2,3], Juan F. Gutiérrez-Bautista[2,3], María C. Barrera-Aguilera[3], Lucía Ballesta[3], Teresa Rodríguez[2,3], María J. Olivares-Durán[2,3] and Francisco Ruiz-Cabello[2,3,4]

1. Servicio de Hematología y Hemoterapia, Hospital Universitario Virgen de las Nieves, Granada, Spain.
2. Instituto de Investigación Biosanitaria de Granada ibs. Granada, Spain.
3. Servicio de Análisis Clínicos e Inmunología, Hospital Universitario Virgen de las Nieves, Granada, Spain.
4. Departamento Bioquímica, Biología Molecular e Inmunología III, University of Granada, Granada, Spain.

Corresponding autor: Mónica Bernal, Servicio de Análisis Clínicos e Inmunología, Hospital Universitario Virgen de las Nieves, Av. De las Fuerzas Armadas, nº2, CP:18014, Granada, Spain. e-mail:monica.bernal.sspa@juntadeandalucia.es. Phone number: +34 958020551

Running title: Cytogenetic landscape of MM revealed by OGM

Keywords: multiple myeloma, optical genome mapping, cytogenetic complexity, structural variants, copy number variations.

Data sharing statement: Data are available upon reasonable request to the corresponding autor.

Author contribution: PJ, JFG, MCB, LB, TR, and MJO collected clinical data, performed and reviewed the diagnostic laboratory tests, and selected the cases included in the study. PG performed the FISH analyses. MB, JP, and JRV conducted the OGM and NGS analyses. JP and MB analyzed the data, drafted the manuscript, and prepared the table and figures. PJ and JRV contributed to the final revision of the manuscript. FRC designed the study, supervised the project, and critically reviewed the manuscript. This work was carried out as part of JP's doctoral thesis.

Conflict of Interest: The authors declare that they have no conflict of interest.

Funding: This work was supported by grants from the Andalusian Government and co-funded by FEDER funds (B-CTS-410–UGR-20 and Group CTS-143), as well as by the Cancer Immunotherapy Network (Red de Inmunoterapia del Cáncer, REINCA).

Acknowledgements: We would like to thank Victoria Calvo and Laura Delgado for their technical assistance.

Multiple myeloma (MM) and its aggressive form, plasma cell leukemia (PCL), are hematological neoplasms characterized by pathological clones of antibody-secreting plasma cells.[1] Currently, next-generation sequencing (NGS) and conventional cytogenetic methods (e.g., karyotyping and fluorescence in situ hybridization (FISH)) are commonly used to identify genetic abnormalities that influence risk stratification.[2,3] However, NGS focuses on detecting variants in the DNA sequence, whereas both karyotyping and FISH are limited in resolution and scope, hindering a comprehensive analysis of the cytogenetic landscape in MM.

Recent research emphasizes the need for better characterization of malignant plasma cells to refine diagnosis, prognosis, and treatment.[4] High-resolution techniques such as Optical Genome Mapping (OGM) offer a more comprehensive approach, enabling genome-wide detection of structural variants (SVs) and copy number variations (CNVs).[5,6]

In this study, OGM, FISH, and karyotyping were employed to analyze chromosomal alterations in a cohort of 21 MM patients and 3 with PCL, alongside NGS for gene mutation analysis. We propose that OGM represents a valuable tool for characterizing the cytogenetic complexity of plasma cells in MM by detecting recurrent, complex, and novel structural alterations with potential prognostic and therapeutic relevance in MM and PCL.

All patients were diagnosed between January 2024 and January 2025 at Hospital Universitario Virgen de las Nieves (Granada, Spain) and met the diagnostic criteria defined by the International Myeloma Working Group (IMWG).[7] MM patients had ≥30% clonal plasma cells in bone marrow, and PCL patients had ≥30% in peripheral blood. Clinical data are summarized in Table 1. All patients gave written informed consent, and the study complied with the Declaration of Helsinki.

OGM was performed on fresh bone marrow or peripheral blood without prior CD138+ cell purification, following Bionano protocols, and analyzed using Bionano Access v1.8 with the Rare Variant Analysis algorithm and the GRCh38 reference genoma. NGS was carried out with a 43-gene panel (Sophia Genetics) on Illumina MiSeq (V3 600-cycle), using DDM software and aligned to GRCh37/hg19. For FISH, CD138+ plasma cells were isolated (autoMACS Pro, Miltenyi Biotec) with >96% purity confirmed by flow cytometry, and key MM alterations were assessed using commercial probes (Metasystems). Conventional karyotyping was performed externally in 16 patients. Of these, 4 had no metaphase growth, 8 showed normal karyotypes but revealed structural and numerical abnormalities by OGM, and 4 exhibited complex karyotypes (Table 1), with OGM offering a more precise characterization, including detection of a cryptic high-risk t(4;14) in one case (*Online Supplementary Figure S1A and Table S1).*

FISH was performed in 22 patients, detecting cytogenetic alterations in 12 (54.5%), while 10 (45.5%) showed no abnormalities. All FISH results were fully concordant with OGM findings (Table 1). However, OGM identified additional chromosomal abnormalities, allowing classification into four levels of cytogenetic complexity. Three patients had Normal profiles, with no significant SVs or CNVs. Five showed Non-Complex profiles (≤3 SVs/CNVs) (Figure 1A). Eleven exhibited Complex profiles (4 to 15 SVs/CNVs), including four with hyperdiploidy (Figure 1B), three with standard risk

translocations such as t(6;14) and t(11;14), and four, two of them with PCL, with high-risk alterations involving chromosome 1 or t(4;14). Finally, five patients, including one with PCL, had Highly Complex profiles, characterized by more than 15 SVs/CNVs and evidence of chromoanagenesis (Figure 1C). Among these, three MM patients and one with PCL carried del(17p) with *TP53* loss, all associated with aggressive or progressive disease. Notably, one MM patient showed extensive chromoanagenesis affecting up to 11 chromosomes but no *TP53* alterations; the only high-risk lesion in this case was a 1q21 gain.

Additionally, we analyzed cytogenetic complexity in one patient at baseline (Figure 2A) and at relapse six months later (Figure 2B). At diagnosis, the patient showed a non-complex profile with three chromosomal rearrangements of uncertain significance. Upon progression, the profile became highly complex, with high-risk alterations including 1q21 gain and 17p deletion (Table 1). Alterations present at diagnosis persisted during disease progression, except for a t(8;11) translocation *(Online Supplementary Table S1).*

OGM revealed additional structural variants (SVs) of uncertain significance, including deletions, insertions, duplications, inversions, and translocations, whose number correlated with cytogenetic complexity: averaging 10 in Normal, 16 in Non-Complex, 27 in Complex, and 57 in Highly Complex profiles. Several SVs involved genes not previously linked to MM but associated with other malignancies. Notably, one patient exhibited a t(X;5) translocation resulting in a *DDX4*::*MAP3K15* fusion, potentially relevant to MM pathogenesis given the role of these genes in cell cycle regulation and tumorigenesis, although functional validation is required *(Online Supplementary Table S1).*

Moreover, NGS was performed in 21 patients to detect variants in 43 MM-related genes. No mutations were identified in four patients, including one with PCL. In the remaining 17, a total of 33 variants were detected across 14 genes, with the most frequently mutated being *KRAS* (n=8), *NRAS* (n=6), *TP53* (n=4), and *ZFHX4* (n=3), all associated with aggressive disease (Table 1). No clear association was observed between overall mutational burden and cytogenetic complexity, except for *TP53* mutations, which were mainly found in patients with Complex or Highly Complex profiles. These *TP53* alterations frequently co-occurred with 17p deletions, resulting in biallelic inactivation, a known marker of poor prognosis and increased risk of relapse.

Our study analyzed cytogenetic profiles of 21 MM and 3 PCL patients with ≥30% pathological plasma cells using OGM, comparing results with FISH and karyotyping. OGM revealed substantial genetic complexity, identifying both well-established MM-associated alterations and novel structural abnormalities of uncertain clinical significance.

Currently, karyotyping, FISH, and NGS are routinely used for diagnosis and risk stratification per international guidelines.[1,8] However, FISH is targeted and does not capture overall genetic complexity, while karyotyping is often uninformative, yielding results in only 30% of cases.[9] In contrast, OGM provided a more precise cytogenetic profile by accurately identifying affected chromosomal regions. Limitations of OGM include difficulty detecting translocations involving entire chromosomal arms (e.g., 1q)

when breakpoints lie in heterochromatic, highly repetitive regions *(Online Supplementary Figure S1).*[10] Importantly, OGM identified the cryptic high-risk t(4;14) not visible by karyotyping, highlighting its value in uncovering hidden alterations that can reclassify patients into high-risk groups.

Our results were fully consistent with FISH for clinically relevant chromosomal alterations, but OGM identified additional CNVs and SVs in all cases. While OGM provides more detailed information, there is no consensus on thresholds defining complex genomic profiles.[11] In B-cell Chronic Lymphocytic Leukemia, a threshold of 10 anomalies has been suggested for highly complex cases, but larger cohort studies are needed to standardize genetic complexity criteria.[12] In our study, OGM allowed us to distinguish different levels of genomic complexity based on the number of anomalies detected. No clear association was found between low complexity and favorable outcomes, highlighting the need for larger cohorts to better characterize these patients. In patients with Complex and Highly Complex genomic profiles, OGM provided more accurate detection of genetic alterations, revealing patterns of hyperdiploidy and chromoanagenesis, which are difficult to fully detect with conventional cytogenetic methods. Hyperdiploidy, found in 50–60% of MM cases, involves trisomies of odd-numbered chromosomes and is linked to better treatment response and prognosis.[13] However, it is not routinely assessed due to the need for multiple FISH probes. Our study showed that OGM reliably identified hyperdiploid cases, providing more precise characterization than standard methods and highlighting its potential for clinical use and improved assessment of hyperdiploidy's prognostic value.

Chromoanagenesis is characterized by multiple catastrophic events, including complex chromosomal rearrangements and copy number alterations, which may affect a few or several chromosomes.[14] OGM technology has provided deeper insights into this phenomenon in hematologic neoplasms,[11,15] highlighting its potential as a poor prognosis marker. In our study, OGM detailed extensive chromosomal rearrangements in patients with chromoanagenesis. Three cases showing biallelic inactivation of *TP53* due to a gene mutation and 17p deletion. In contrast, a fourth patient with a complex profile but without evidence of chromoanagenesis, showed only the 17p deletion. These findings suggest that a double hit on *TP53* may be required to promote the accumulation of complex chromosomal rearrangements, aligning with the hypothesis recently proposed in a study of the chromoanagenesis in patients with Acute Myeloid Leukemia.[16] Given this, further studies are necessary to better understand the mechanisms underlying chromoanagenesis, its relationship with *TP53* status, and its impact on disease progression. In this context, OGM proves to be the most effective tool for investigating this complex cytogenetic phenomenon.

Our study included three patients with PCL: two in advanced disease stages and one diagnosed de novo (Table 1). All showed complex or highly complex cytogenetic profiles with high-risk alterations typical of PCL. Notably, one case exhibited chromoanagenesis with biallelic *TP53* inactivation. However, larger cohorts are needed to precisely characterize the cytogenetic profile of this aggressive disease form.

Additionally, we used OGM to analyze chromosomal alterations in a MM patient at diagnosis and relapse, observing a shift from a Non-complex to a Highly Complex

profile with acquisition of 17p deletion and 1q21 gain. We also observed the loss of an unreported t(8;11) at relapse, possibly reflecting the sucblonal regression. Multiple myeloma is characterized by genetically distinct subclones that respond independently to treatment and contribute to disease progression.[17] OGM detects structural variants beyond known high-risk alterations, which could aid in capturing subclonal dynamics. However, its sensitivity is limited, and further studies are needed to clarify OGM's role in disease monitoring and its potential clinical relevance.

This study revealed numerous structural variants of uncertain significance (VUS), whose biological relevance remains unclear. Ongoing analyses using advanced bioinformatic tools aim to assess their recurrence and potential clinical impact.

NGS proved valuable for identifying mutations in genes that may serve as novel therapeutic targets in MM and support patient enrollment in clinical trials.[18] Importantly, NGS detects mutations in *TP53*, a key high-risk gene, enabling a more complete assessment of biallelic inactivation. Unlike FISH, which only detects 17p deletions, NGS reveals point mutations and small indels. Thus, integrating NGS with cytogenetic analyses provides critical molecular insights that influence prognosis and guide targeted therapies.

This study has some limitations, including the lack of external validation for additional alterations and the small cohort size. Additionally, patients with ≥30% pathological plasma cell infiltration were selected to ensure a homogeneous group and sufficient tumor burden, as OGM has limited sensitivity for CNVs. To clarify whether these findings extend to cases with lower infiltration, OGM is now being applied to purified CD138+ plasma cells, aiming to improve genomic characterization in patients with low tumor burden or at the MGUS–MM transition.

In conclusion, OGM may play a key role in unraveling the cytogenetic complexity of plasma cells and capturing their unique genomic "fingerprint". Combined with NGS, it significantly enhances MM genetic characterization by enabling the detection of both structural and sequence-level alterations. This integrated approach improves the identification of high-risk features such as biallelic *TP53* inactivation, hyperdiploidy, and chromoanagenesis. While the MM genomic landscape remains incompletely defined, these technologies are expected to improve diagnosis, risk stratification, and treatment decisions.

References

1. Rajkumar SV. Multiple myeloma: 2024 update on diagnosis, risk-stratification, and management. Am J Hematol. 2024;99(9):1802-1824.
2. Kumar SK, Rajkumar SV. The multiple myelomas - current concepts in cytogenetic classification and therapy. Nat Rev Clin Oncol. 2018;15(7):409-421.
3. Munawar U, Rasche L, Muller N, et al. Hierarchy of mono- and biallelic TP53 alterations in multiple myeloma cell fitness. Blood. 2019;134(10):836-840.
4. Rodriguez-Otero P, Paiva B, San-Miguel JF. Roadmap to cure multiple myeloma. Cancer Treat Rev. 2021;100:102284.
5. Giguère A, Raymond-Bouchard I, Collin V, Claveau JS, Hébert J, LeBlanc R. Optical Genome Mapping Reveals the Complex Genetic Landscape of Myeloma. Cancers (Basel). 2023;15(19):4687.
6. Zou YS, Klausner M, Ghabrial J, et al. A comprehensive approach to evaluate genetic abnormalities in multiple myeloma using optical genome mapping. Blood Cancer J. 2024;14(1):78.
7. Rajkumar SV, Dimopoulos MA, Palumbo A, et al. International myeloma working group updated criteria for the diagnosis of multiple myeloma. Lancet Oncol. 2014;15(12):e538-e548.
8. Caers J, Garderet L, Kortüm KM, et al. European Myeloma Network recommendations on tools for the diagnosis and monitoring of multiple myeloma: what to use and when. Haematologica. 2018;103(11):1772-1784.
9. Gutensohn K, Weh HJ, Walter TA, Hossfeld DK. Cytogenetics in multiple myeloma and plasma cell leukemia: simultaneous cytogenetic and cytologic studies in 51 patients. Ann Hematol. 1992;65(2):88-90.
10. Puiggros A, Mallo M, Díaz-González A, et al. Optical genoma mapping: technical basis and applications in hematological malignancies. Sangre (Eng). 2023;42(2):77-91.
11. Yang H, Garcia-Manero G, Sasaki K, et al. High-resolution structural variant profiling of myelodysplastic syndromes by optical genome mapping uncovers cryptic aberrations of prognostic and therapeutic significance. Leukemia. 2022;36(9):2306-2316.
12. Puiggros A, Ramos-Campoy S, Kamaso J, et al. Optical genome mapping: a promising new tool to assess genomic complexity in chronic lymphocytic leukemia (CLL). Cancers (Basel). 2022;14(14):3376.
13. Manier S, Salem KZ, Park J, Landau DA, Getz G, Ghobrial IM. Genomic complexity of multiple myeloma and its clinical implications. Nat Rev Clin Oncol. 2017;14(2):100-113.
14. Holland AJ, Cleveland DW. Chromoanagenesis and cancer: mechanisms and consequences of localized, complex chromosomal rearrangements. Nat Med. 2012;18(12):1630-1638.
15. Guermouche H, Roynard P, Servoli F, et al. Deciphering Genomic Complexity of Multiple Myeloma Using Optimized Optical Genome Mapping. J Mol Diagn. 2025;27(4):306-322.

16. Wei Q, Hu S, Loghavi S, et al. Chromoanagenesis is frequently associated with highly complex karyotypes, extensive clonal heterogeneity, and treatment refractoriness in acute myeloid leukemia. Am J Hematol. 2025;100(3):417-426.
17. Sandmann S, Karsch K, Bartel P, et al. The role of clonal evolution on progression, blood parameters, and response to therapy in multiple myeloma. Front Oncol. 2022;12:919278.
18. Walker BA, Mavrommatis K, Wardell CP, et al. Identification of novel mutational drivers reveals oncogene dependencies in multiple myeloma. Blood. 2018;132(6):587-597.

Table 1. Clinical Data and summary of results from Next Generation Sequencing, karyotyping, Fluorescence *In Situ* Hybridization and Optical Genome Mapping.

MM Patient	Sex	Age	Diagnosis	PC %*	NGS Mutated Gen (VAF)	Karyotype	FISH**	OGM HR alteration† Cytogenetic profile‡
1	M	75	Kappa IgA	40	*TENT5C* (2%)	N/A	NORMAL	NO HR alterations Normal profile
2	F	59	Kappa IgA	30	N/A	No dividing cells	NORMAL	NO HR alterations Normal profile
3	M	65	Kappa IgG	31	ND	NORMAL	NORMAL	NO HR alterations Normal profile
4	F	47	Lambda IgG	33	*ZFHX4* (23%), *KRAS* (5%), *NRAS* (3%)	NORMAL	NORMAL	NO HR alterations Non-Complex profile
5	M	73	Kappa IgG	31	*CYLD (8%),* *ZFHX4* (7%), *FAT3* (7%)	N/A	NORMAL	NO HR alterations Non-Complex profile.
6	M	70	Progressing Lambda IgA	49	N/A	No dividing cells	1q21 gain	1q21 gain Non-Complex profile.
7	M	82	Kappa IgA	60	*DUSP2* (18%)	N/A	1q21 gain,	1q21 gain Non-Complex profile.
8	M	75	Kappa IgG	44	*TRAF3* (5%) *KRAS* (4%)	NORMAL	1p32 deletion 1q21 gain	1p32 deletion, 1q21 gain Non-Complex profile.
9	M	78	Lambda free light chain	90	*NRAS* (13%)	No dividing cells	NORMAL	NO HR alterations Complex profile.
10	M	56	Kappa IgG	32	*NRAS* (7%)	NORMAL	NORMAL	NO HR alterations Complex profile (hyperdiploidy)
11	M	45	Kappa IgG	95	ND	NORMAL	NORMAL	NO HR alterations Complex profile (hyperdiploidy)
12	M	56	Lambda free light chain	76	*TRAF3* (13%) *LTB* (11%)	COMPLEX	NORMAL	NO HR alterations Complex profile (hyperdiploidy)
13	M	87	Kappa IgA	33	*KRAS* (13%)	N/A	NORMAL	NO HR alterations Complex profile (hyperdiploidy)
14	F	77	Lambda IgG	70	*KRAS* (36%) *NRAS* (46%)	NORMAL	*CCND1::IGH*	NO HR alterations, Complex profile (chromoanagenesis, *CCND1::IGH*)
15	M	66	Kappa IgG	32	N/A	NORMAL	1p32 deletion	1p32 deletion Complex profile.
16	M	64	Kappa IgA	30	*TP53* (24%) *CCND1* (31%)	N/A	1q21 gain *CCND1::IGH*	1q21 gain Complex profile (*CCND1::IGH*)
17	M	64	Lambda IgG	30	ND	N/A	1p32 deletion 1q21 gain	1p32 deletion, 1q21 gain. Complex profile.
18	M	79	Lambda IgA	81	*KRAS* (19%)	N/A	1q21 gain *CCND1::IGH*	1q21 gain, Highly Complex profile (chromoanagenesis, *CCND1::IGH*)
19	M	76	Progressing Lambda IgA	70	*TP53* (8%)	No dividing cells	N/A	17p deletion. Highly Complex profile (chromoanagenesis)
20	M	49	Progressing Lambda IgG	96	*TP53* (86%) *ZFHX4* (44%)	NORMAL	1p32 deletion 1q21 gain 17p deletion	1p32 deletion, 1q21 gain, 17p deletion. Highly Complex profile (hyperdiploidy and chromoanagenesis)
21[a]	M	63	Basal Kappa IgA	60	*NRAS* (4%) *RB1* (3%)	N/A	NORMAL	NO HR alterations Non-Complex profile.
21[b]			Progressing Kappa IgA	35	*NRAS* (27%) *RB1* (33%)	COMPLEX	1q21 gain 17p deletion	1q21 gain, 17p deletion. Highly Complex profile.
LCP Patient	**Sex**	**Age**	**Diagnosis**	**PC %***	**NGS** Mutated Gen (VAF)	**Karyotype**	**FISH****	**OGM** HR alteration† Cytogenetic profile‡
22	M	36	De novo Kappa IgG	80	*DIS3* (39%), *CYLD* (25%), *KRAS* (7%) *KRAS* (5%), *BRAF* (4%)	N/A	1q21 gain	1q21 gain. Complex profile.
23	F	63	Progressing Lambda IgG	43	ND	COMPLEX	1q21 gain *FGFR3::IGH*	1q21 gain, *FGFR3::IGH* Complex profile.
24	M	73	Progressing Lambda Free Light Chain	60	*TP53* (64%), *KRAS* (38%), *TENT5C* (15%)	NORMAL	N/A	1p32 deletion, 17p deletion. Highly Complex profile (chromoanagenesis)

MM: Multiple Myeloma; **PCL**: Plasma Cell Leukemia; **PC**: Plasma cell; **NGS:** Next Generation Sequencing; **VAF**: Variant Allele Frequency; **FISH**: Fluorescence *In Situ* Hybridization; **OGM**: Optical Genome Mapping; **F:** Female; **M:** Male**; HR:** High-Risk; **N/A**: Not Available; **ND:** Not Detected.

***** % plasma cells observed in the morphological study of bone marrow aspirate (MM) or peripheral blood (PCL).

****** In the FISH study, probes were used to analyze recurrent and/or clinically relevant alterations: t(4;14), *FGFR3::IGH*; t(11;14) *CCND1::IGH*; and t(14;16), *IGH::MAF*; as well as 17p13 deletion (*TP53*), 1p32 deletion (*CDKN2C*), and 1q21 gain (*CKS1B*).

† High-Risk chromosomal anomalies: t(4;14), t(14;16), t(14;20), 1q21 gain, 1p32 deletion, and 17p deletion.

‡ Classification of the cytogenetic profile: Normal (no significant stuctural variants (SVs) or copy number variations (CNVs) detected), Non-Complex (≤3 SVs/CNVs detected), Complex (4-15 SVs/CNVs detected), Highly COmplex (>15 SVs/CNVs detected with or without the presence of chromoanagenesis).

[a,b] Results from the same patient with Kappa IgA MM (patient #21) obtained at baseline (a) and at the time of progression six months later (b).

Figure Legends:

Figure 1. Optical genome mapping (OGM) results illustrating different cytogenetic complexity profiles (left: *Circos plot*; right: *Whole Genome*).
(A) Patient #7 with a Non-Complex cytogenetic profile (≤3 structual variants (SVs)/copy number variations (CNVs) detected), showing 1q gain as the only high-risk alteration. **(B)** Patient #13 with a Complex profile (4–15 SVs/CNVs detected), characterized by hyperdiploidy (trisomies of chromosomes 3, 5, 7, 9, 11, 15, 17, and 19), with no high-risk alterations identified. **(C)** Patient #18 with a Highly Complex profile (>15 SVs/CNVs detected), displaying multiple rearrangements affecting nearly all chromosomes, indicative of chromoanagenesis. High-risk 1q gain was detected, along with standard-risk alterations such as the t(11;14) translocation.
SVs<1 Mb were filtered out from the *Circos plot* unless involving clinically significant regions. The *Whole Genome* view enables visualization of CNVs in the analyzed sample (gains in blue and losses in red)

Figure 2. Optical Genome Mapping (OGM) reveals the acquisition of chromosomal alterations during disease progression in patient #21 (left: *Circos plot;* **right:** *Whole Genome).*
(A) Chromosomal alterations detected at the time of diagnosis. **(B)** Chromosomal profile during disease progression six months later. At diagnosis (A), a non-complex cytogenetic profile was observed, characterized by a translocation between chromosomes X and 5 along with subclonal alterations involving translocations between chromosomes 2 and 8 and between chromosomes 8 and 11. At disease progression (B), a highly complex cytogenetic profile was detected, marked by the acquisition of high-risk alterations, including a 1q21 gain and 17p deletion. Additional abnormalities included trisomies of chromosomes 7 and 9; monosomies of chromosomes 4 and 13; gains in regions of chromosomes 2, 3, 5, 6, 8, and 19; a deletion in the long arm of chromosome 16; and translocations between chromosomes 6 and 8 (t(6;8)) and between chromosomes 16 and 17 (t(16;17)), the latter associated with 17p loss. Previously identified alterations were still detectable: the t(X;5) and the t(2;8). In contrast, the t(8;11) translocation detected at diagnosis was no longer present, suggesting the regression of a minor cellular subclone.

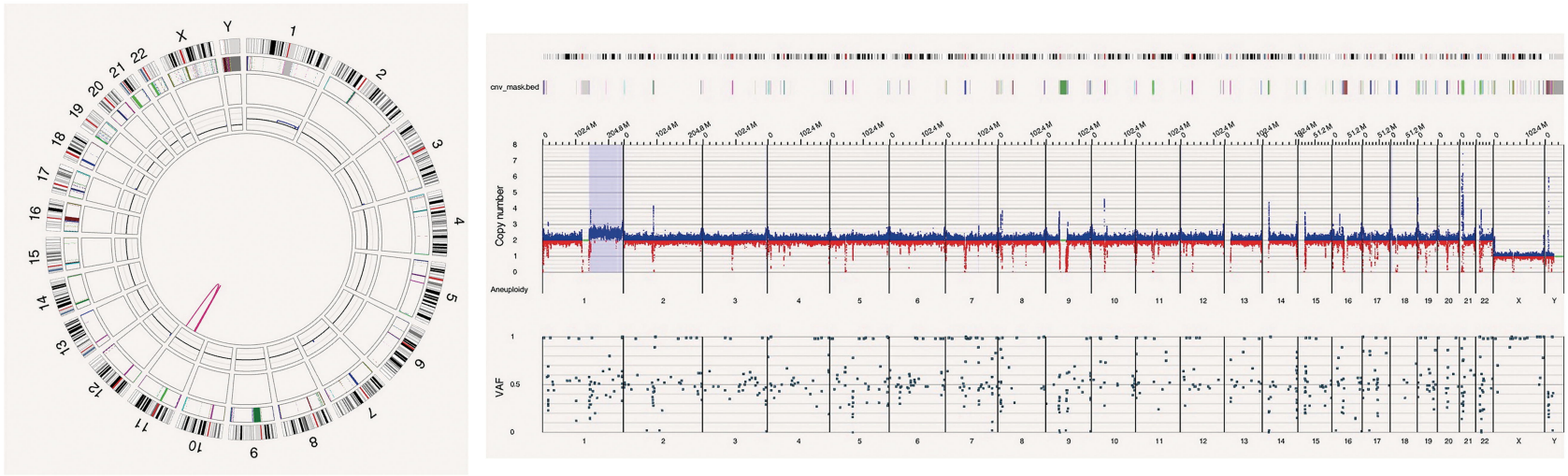
A
cnv_mask.bed
Copy number
Aneuploidy
VAF

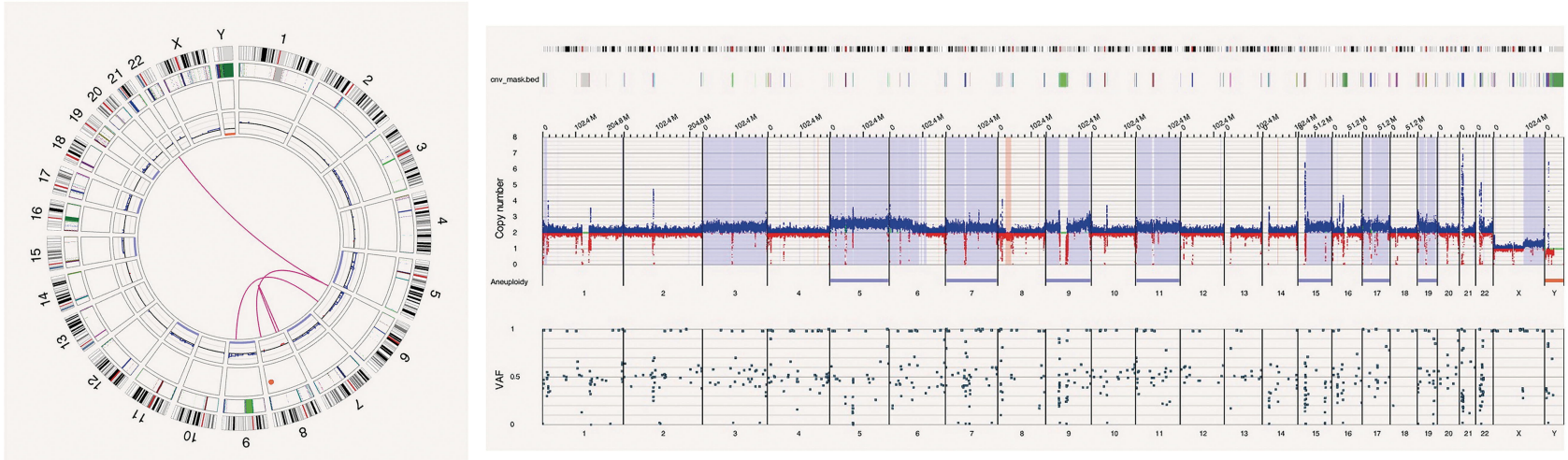
B
cnv_mask.bed
Copy number
Aneuploidy
VAF

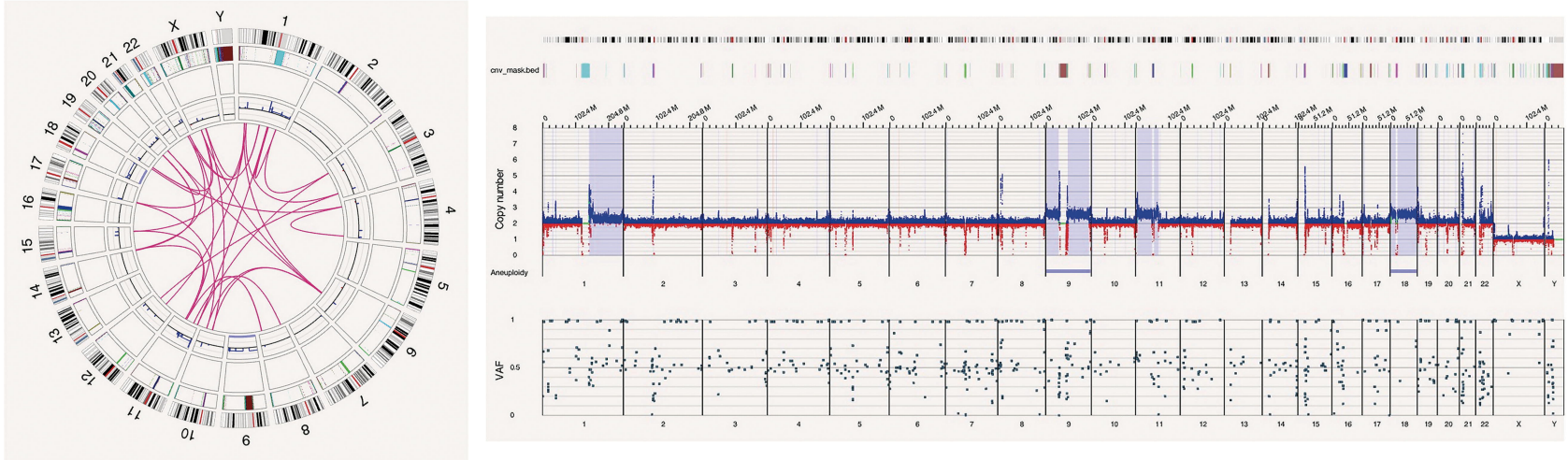
C
cnv_mask.bed
Copy number
Aneuploidy
VAF

A

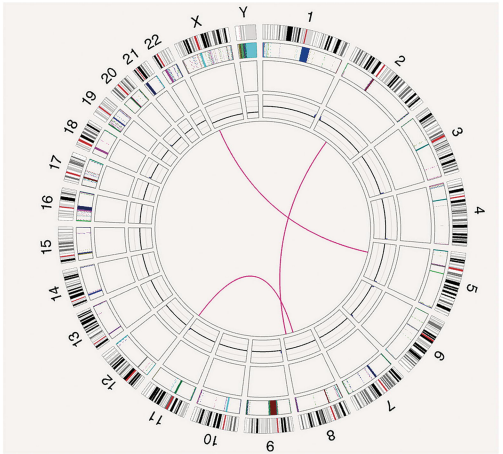
X
Y
1
2
3
4
5
6
7
8
9
10
11
12
13
14
15
16
17
18
19
20
21
22

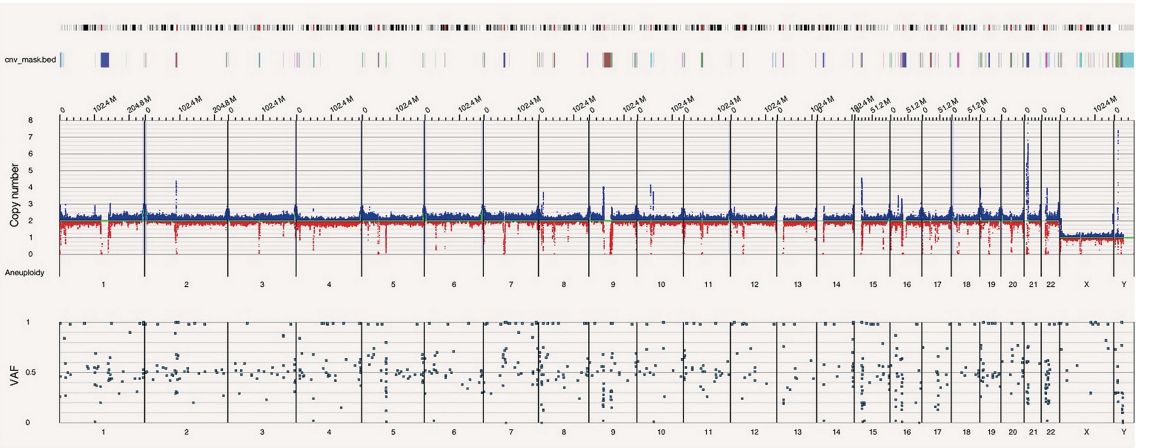
cnv_mask.bed
Copy number
Aneuploidy
VAF
1
2
3
4
5
6
7
8
9
10
11
12
13
14
15
16
17
18
19
20
21
22
X
Y

B

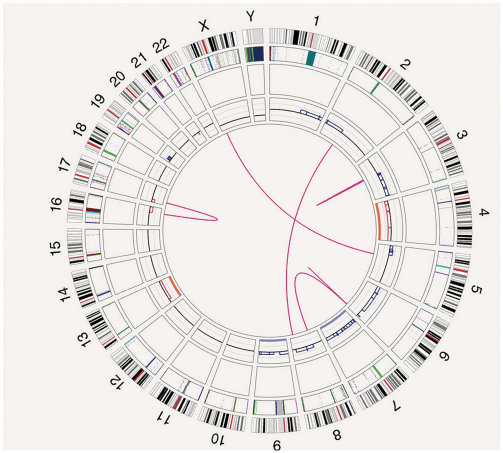
X
Y
1
2
3
4
5
6
7
8
9
10
11
12
13
14
15
16
17
18
19
20
21
22

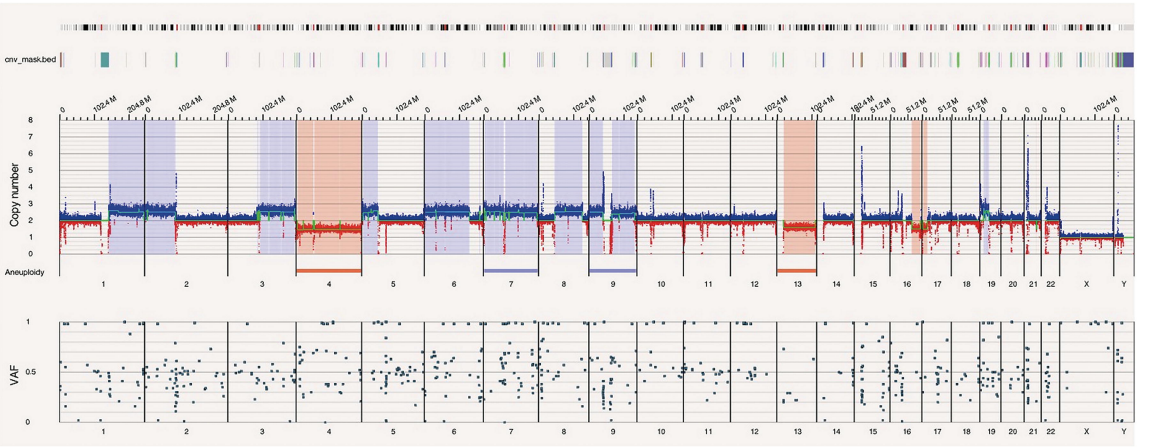
cnv_mask.bed
Copy number
Aneuploidy
VAF
1
2
3
4
5
6
7
8
9
10
11
12
13
14
15
16
17
18
19
20
21
22
X
Y

Supplementary Table S1. Detailed Results from Next Generation Sequencing, Karyotyping, Fluorescence *In Situ* Hybridization, and Optical Genome Mapping

MM Patient	NGS Gene Variant (VAF)	Karyotype	FISH*	OGM HR alterations/Classification of the cytogenetic profile‡ SVs/CNVs (ISCN 2024)†§
1	***TENT5C*** p.K128Nfs*22 (2%)	N/A	NORMAL	NO high-risk alterations identified **NORMAL** cytogenetic profile
2	N/A	No dividing cells	NORMAL	NO high-risk alterations identified. **NORMAL** cytogenetic profile
3	ND	NORMAL	NORMAL	NO high-risk alterations identified. **NORMAL** cytogenetic profile
4	***ZFHX4*** p.S2062Cfs*77 (23%) ***KRAS*** p.G13D (5%) ***NRAS*** p.Q61K (3%)	NORMAL	NORMAL	NO high-risk alterations identified. **NON-COMPLEX** cytogenetic profile with **hyperdiploidy** (ogm (9)x3[0.26],(15)x3[0.16],(19)x3[0.19])
5	***CYLD*** p.W847* (8%), ***ZFHX4*** p.A3245V (7%) ***FAT3*** p.E2048K (7%)	N/A	NORMAL	NO high-risk alterations identified. **NON-COMPLEX** cytogenetic profile. (ogm[GRCh38] 9q21.11q34.2(67018228_133526602)x3[0.19], 13q14.3q34.3(52185900_110867008)x1[0.2])
6	N/A	No dividing cells	1q21 gain	High-risk alterations identified: **1q21 gain.** **NON-COMPLEX** cytogenetic profile. (ogm[GRCh38] 1q21.1q44(144294282_248943333)x3[0.2],8p23.1p12(8158967_36285880)x1[0.2])
7	***DUSP2*** p.V224A (18%)	N/A	1q21 gain,	High-risk alterations identified: **1q21 gain.** **NON-COMPLEX** cytogenetic profile. (ogm[GRCh38] 1q21.1q44(144080779_248943333)x3[0.3],t(11;11)(q13.1;q13.3)(64406822;70013323)[0.21],t(11;11)(q13.1;q23.3)(65861642;120576312)[0.13])
8	***TRAF3*** p.K436Nfs*17 (5%) ***KRAS*** p.G12A (4%)	NORMAL	1p32 deletion 1q21 gain	High-risk alterations identified: **1p32 deletion, 1q21 gain.** **NON-COMPLEX** cytogenetic profile. (ogm[GRCh38] 1p33p32.3(49103054_50903109)x1[0.2],1q21.1q21.2(143278152_148928812)x3[0.3],13q21.1q33.3(57628403_107673930)x1[0.17])
9	***NRAS*** p.Q61R (13%)	No dividing cells	NORMAL	NO high-risk alterations identified. **COMPLEX** cytogenetic profile. (ogm[GRCh38] t(6;14)(p21.1;q32.33)(41973240;105710125)[0.36], 6p21.1p11.2(41974762_58445657)x1[0.3],9q33.1q34.11(117729225_130596749)x3[0.2], (13)x1[0.3],(14)x1[0.3],16q11.1q23.3(38277017_82690601)x1[0.3])
10	***NRAS*** p.Q61H (7%)	NORMAL	NORMAL	NO high-risk alterations identified. **COMPLEX** cytogenetic profile with **hyperdiploidy.** (ogm (5)x3[0.2],(9)x3[0.3],(11)x3[0.3],(15)x3[0.2],(19)x3[0.16],(21)x3[0.16])
11	ND	NORMAL	NORMAL	NO high-risk alterations identified. **COMPLEX** cytogenetic profile with **hyperdiploidy.** (ogm[GRCh38] t(X;3)(q27.3;p26.3)(12920;143474934)[0.56], t(1;8)(p22.2;p11.21)(90183393;41042182)[0.11],1p22.2p12(90469199_120191913)x1[0.3], t(1;22)(q23.3;q13.1)(161777800;38687685)[0.09],(3)x3[0.2],t(4;5)(p16.3;q14.3)(1901670;88835964)[0.13],5q14q35.3(88845196_181472714)x3[0.2], (7)x3[0.4],8p23.2p11.1(3935347_41156020)x1[0.25],9q21.11q34.2(65322076_133526602)x3[0.2],(11)x3[0.2],(14)x1[0.3],(15)x3[0.2], t(17;20)(q21.31;q13.13)(45283546;49126484)[0.08],(19)x3[0.2])
12	***TRAF3*** p.E271* (13%) ***LTB*** c.163-1G>A (11%)	55,XY,+2,+5,+7,+9,+11, -14,+15,+15,+19,+21, +mar[6]/46,XY[24]).	NORMAL	NO high-risk alterations identified. **COMPLEX** cytogenetic profile with **hyperdiploidy.** (ogm[GRCh38] (2)x3[0.3],(5)x3[0.7],6p25.3q27(76216_169967990)x3[0.3],t(6;14)(q21;q23.3)(106247425;65375083)[0.18],(7)x3[0.4],(9)x3[0.2],(11)x3[0.5], 14q23.3q32.31(65352855_102165030)x1[0.4],(15)x3[0.6],(19)x3[0.5],(21)x3[0.3])
13	***KRAS*** p.G12C (13%)	N/A	NORMAL	NO high-risk alterations identified. **COMPLEX** cytogenetic profile with **hyperdiploidy.** (ogm[GRCh38] Xq21.31q28(92477611_155695743)x2[0.6],(Y)x0[0.3],(3)x3[0.2],(5)x3[0.5],6p25.3q13(76216_69646176)x3[0.4], t(6;8)(p24.3;q24.21)(8750925;127741499)[0.17], t(6;21)(p24.3;q21.3)(8756616;29321555)[0.12],t(6;9)(q21;q31.1)(113958488;103806436)[0.14],(7)x3[0.2], 8p21.3p12(22305520_35035604)x1[0.3],(9)x3[0.2],(11)x3[0.2],(15)x3[0.2],(17)x3[0.3],(19)x3[0.2])

Supplementary Table S1. Detailed Results from Next Generation Sequencing, Karyotyping, Fluorescence *In Situ* Hybridization, and Optical Genome Mapping (continued)

MM Patient	NGS Gene Variant (VAF)	Karyotype	FISH*	OGM HR alterations/Classification of the cytogenetic profile‡ SVs/CNVs (ISCN 2024)†§
14	***KRAS*** p.G12C (13%)	N/A	NORMAL	NO high-risk alterations identified. **COMPLEX** cytogenetic profile with **hyperdiploidy.** (ogm[GRCh38] Xq21.31q28(92477611_155695743)x2[0.6], (Y)x0[0.3],(3)x3[0.2],(5)x3[0.5],6p25.3q13(76216_69646176)x3[0.4], t(6;8)(p24.3;q24.21)(8750925;127741499)[0.17], t(6;21)(p24.3;q21.3)(8756616;29321555)[0.12],t(6;9)(q21;q31.1)(113958488;103806436)[0.14], (7)x3[0.2],8p21.3p12(22305520_35035604)x1[0.3],(9)x3[0.2],(11)x3[0.2],(15)x3[0.2],(17)x3[0.3],(19)x3[0.2])
15	N/A	NORMAL	1p32 deletion	High-risk alterations identified: **1p32 deletion.** **COMPLEX** cytogenetic profile. (ogm[GRCh38] 1p33p21.1(47726928_105547900)x1[0.16],6p11.1q27(59282244_167047482)x1[0.16],t(6;20)(q14.1;q11.1)(76543631;29866072)[0.05],(15)x3[0.25])
16	***TP53*** Y220C (24%) ***CCND1*** p.Y44H (31%)	N/A	1q21 gain *CCND1::IGH*	High-risk alterations identified: **1q21 gain.** **COMPLEX** cytogenetic profile. (ogm[GRCh38] 1q21.1q44(145439805_248943333)x3[0.3],3p24.3p11(19114300_89780698)x1[0.3],t(5;8)(q33.3;q24.21)(156787070;127808529)[0.24], 8p23.2p12(2696469_34845069)x1[0.4],t(8;11)(p12;q12.3)(34857598;63447000)[0.11],t(11;14)(q13.3;q32.33)(69453684;105887565)[0.4], (13)x1[0.4],14q22.2q24.3(54824875_74983142)x1[0.4],16q11.1q24.1(38277017_85265163)x1[0.4])
17	ND	N/A	1p32 deletion 1q21 gain	High-risk alterations identified: **1p32 deletion, 1q21 gain.** **COMPLEX** cytogenetic profile. (ogm[GRCh38] Xq21.3q28(26047969_155695743)x2[0.1],(Y)x0[0.3],1p32.3(50750291_50991589)x1[0.1],1q21.1q23.3(144349979_161410556)x3[0.2], (4)x1[0.25],5p15.32p11(4889453_46400789)x3[0.25],13p11.1q14.3(17542017_53293428)x3[0.16],(19)x3[0.25])
18	***KRAS*** p.G13D (19%)	N/A	1q21 gain *CCND1::IGH*	High-risk alteration identified: **1q21 gain.** **HIGHLY COMPLEX** cytogenetic profile with **chromoanagenesis** affecting chromosomes X, 1, 3, 6, 8, 10, 11, 12, 14, 15, 17, 19, 20 and 22. The t(11;14) (*CCND1::IGH*) translocation is detected, along with numerous CNVs (gains) associated with the rearrangement breakpoints and trisomies of chromosomes 9 and 18.
19	***TP53*** p.V216M (8%)	No dividing cells	N/A	High-risk alterations identified: **17p deletion.** **HIGHLY COMPLEX** cytogenetic profile with **chromoanagenesis** affecting chromosomes 9, 12 and 15. (ogm[GRCh38] Xq23q28(113114252_155695743)x2[0.3],3p26.3q29(12920_195582326)x3[0.3],t(3;13)(p24.1;q21.1)(29318793;58877056), 4p16.1p13(7777952_42154587)x1[0.2],8p23.1q12.1(7685458_58265497)x3[0.2],8q24.13q24.3(123105050_141829244)x3[0.2],9p24.3p13.1(3997523_38885219)x3[0.2],t(9;9)(q21.11;q22.32)(69050405;94579639)[0.11],t(9;9)(q22.33;q34.12)(97250381;130692700)[0.13],(11)x3[0.3],t(12;12)(p13.1;q12)(13082454;41026558)[0.1],t(12;12)(q12 ;q13.13)(40964700;51695910)[0.1],t(15;15)(q12;q14)(26477223;36411226)[0.05],t(15;15)(q14;q21.3)(34258611;56714294)[0.12],17p13.1(7562929_7865216)x1[0.14],22q 11.23q12.3(25306236_33779120)x1[0.2])
20	***TP53*** p.R273C (86%) ***ZFHX4*** p.Y240* (44%)	NORMAL	1p32 deletion 1q21 gain 17p deletion	High-risk alterations identified: **1p32 deletion, 1q21 gain, 17p deletion.** **HIGHLY COMPLEX** cytogenetic profile with **hyperdiploidy** and **chromoanagenesis** affecting chromosomes 2 and 4. (ogm[GRCh38] Xq22.1q28(101912108_ 153085624)x2[0.2],t(1;17)(p36.21;q22)(14970717;59155199)[0.25],1p34.3p11.2(39493048_121608073)x1, 1q21.1q44(143278152_248943333)x3,t(1;2)(q43;p23.2)(243471142;29317751)[0.39], t(2;14)(p23.2;q32.11)(29222051;91322093)[0.47], t(2;2)(p23.1;p21)(30104027;47489559)[0.46],(3)x3[0.7],(4)x3[0.3],t(4;4)(q13.1;q21.1)(63907330;75894412)[0.06], t(4;4)(q21.1;q26)(76997597;116133956)[0.1],(5)x3[0.8],(6)x3[0.8],(7)x3[0.8],9q21.11q34.2(68310629_133526602)x3[0.3],(11)x3[0.8],(15)x3[0.8], 16p13.3(3051463_ 35562558)x3[0.8],17p13.1p11.2(9531696_16197684)x1[0.2], (19)x3[0.7],(21)x3[0.9])
21[a]	***NRAS*** p.Q61H (3.7%) ***RB1*** p.F336Sfs* (3.2%)	N/A	NORMAL	NO high-risk alterations identified. **NON-COMPLEX** cytogenetic profile. (ogm[GRCh38] t(X;5)(p22.12;q11.2)(55805207;19402072)[0.42],t(2;8)(p11.2;q24.21)(88623796;128150396)[0.06],t(8;11)(q21.3;q25)(90787268;135061119)[0.06])
21[b]	***NRAS*** p.Q61H (27%) ***RB1*** p.F336Sfs* (33%)	48,XY,t(2;8)(p13;q24), +3,del(3)(p13),-4,+6, add(6)(q27),del(6)(q23), +7,+9,der(9)t(1;9) (q12;p22),-13, dic(16;17)(q21;p13), -17,+mar[20]	1q21 gain 17p deletion	High-risk alterations identified: **1q21 gain, 17p deletion.** **HIGHLY COMPLEX** cytogenetic profile. (ogm[GRCh38] t(X;5)(p22.12;q11.2)(55805207;19403196)[0.5],1q21.1q44(144117875_248633312)x3[0.5],2p25.3p11.2(15924_88827954)x3[0.5], t(2;8)(p11.2;q24.21)(88623796;128139663)[0.16],t(3;3)(p12.3;p12.1)(78395759;83866294)[0.23],3q11.1q29(93819201_198230596)x3[0.5],(4)x1[0.6], 5p15.33p11(2186408_46118384)x3[0.5],6p25.3q26(76216_163053979)x3[0.5],t(6;6)(q26;q26)(161311088;161681393)[0.24], t(6;8)(q26;q11.1)(163057787;46376653)[0.21],(7)x3[0.5],8q11.1q24.1(45972483_127958936)x3[0.5],(9)x3[0.4],(13)x1[0.45],16q21q24.2(62505702_88143333)x1[0.5], t(16;17)(q21;p12)(62587688;14289017)[0.26],17p13.3p12(1315080_14305528)x1[0.5],19p13.2p11(9090781_ 24420459)x3[0.6])

Supplementary Table S1. Detailed Results from Next Generation Sequencing, Karyotyping, Fluorescence *In Situ* Hybridization, and Optical Genome Mapping (continued)

LCP Patient	NGS Gene Variant (VAF)	Karyotype	FISH*	OGM HR alterations†/Classification of the cytogenetic profile‡ SVs/CNVs (ISCN 2024)§
22	***DIS3*** p.D488N (39%) ***CYLD*** p.S409* (25%) ***KRAS*** p.G12R (67%) ***KRAS*** p.A59E (5%) ***BRAF*** p.G469A (4%)	N/A	1q21 gain	High-risk alterations identified: **1q21 gain.** **COMPLEX** cytogenetic profile. (ogm[GRCh38] t(X;10)(q27.3;p12.33)(18,215,572;145,450,166)[0.51],Xq27.3q28(145,473,969_155,695,747)x2[0.25],1q21.1q44(143278152_248642991)x3[0.2], 10p15.3p12.33(18514_6242295)x1[0.7],t(11;14)(q13.3;q32.33)(69511003;106340554)[0.44],11q13.3q25(68975206_135069565)x3[0.7])
23	ND	43,X,-X,+3, add(6)(q13), -11, -12,-13, add(16)(q24),-20, +mar[9]/43,sl, der(8)t(1;8)(q21;p23)[9] /43,sdl1,add(22)(p13)[2]/ 43,sdl2,der(17)t(1;17)(q2 1;p13)[3]/46,XX[2]	1q21 gain *FGFR3::IGH*	High-risk alterations identified: **1q21 gain, *FGFR3*::*IGH* (t(4;14)).** **COMPLEX** cytogenetic profile. (ogm[GRCh38] (X)x1[0.5],1q21.1q44(144293458_248304428)x3[0.4],(3)x3[0.5],t(4;14)(p16.3;q32.33)(1883975;106365267)[0.27], 6q12q27(68295166_167058007)x1[0.5],t(6;7)(q12;q21.12)(68295166;87457043)[0.23],7q11.23q36.3(77693781_158044213)x3[0.4], t(11;11)(q12.1;q22.3)(56028409;109141119)[0.21],11q14.1q22.3(85479021_104641634)x1[0.5],12p13.32q13.12(4271654_51023363)x1[0.6], t(12;20)(q13.12;p11.21)(51055371;22714750)[0.26],(13)x1[0.6],16q11.2q23.3(46478822_83057720)x1[0.5],20p13p11.21(3413731_22796609)x1[0.5])
24	***TP53*** p.R273H (64%) ***KRAS*** p.G12S (38%) ***TENT5C*** p.F177Lfs*34 (15%)	NORMAL	N/A	High-risk alterations identified**: 1p32 deletion, 17p deletion.** **HIGHLY COMPLEX** cytogenetic profile with **chromoanagenesis** events affecting chromosomes X, 3, 5, 8, 11, 13 and 22. Additional rearrangements, CNVs associated with translocation breakpoints, trisomies of chromosomes 9, 14, and 19, as well as monosomy of chromosome 13, are observed.

NGS: Next Generation Sequencing; **VAF**: Variant Allele Frequency; **FISH**: Fluorescence *In Situ* Hybridization; **OGM**: Optical Genome Mapping; **HR:**High-Risk; **SV**: Structural Variant; **CNV**:Copy Number Variant; **ISCN**: International System for Human Cytogenetic Nomenclature 2024; **MM**: Multiple Myeloma; **PCL**: Plasma Cell Leukemia, **N/A**: Not Available; **ND:** Not Detected.

***** In the FISH study, probes were used to analyze recurrent and/or clinically relevant alterations: t(4;14), *FGFR3::IGH*; t(11;14) *CCND1::IGH*; and t(14;16), *IGH::MAF*; as well as 17p13 deletion (*TP53*), 1p32 deletion (*CDKN2C*), and 1q21 gain (*CKS1B*).

† HR alterations: t(4;14), t(14;16), t(14;20), 1q21 gain, 1p32 deletion, and 17p deletion.

‡ Classification of the cytogenetic profile: NORMAL (no significant SVs or CNVs detected), NON-COMPLEX (≤3 SVs/CNVs detected), COMPLEX (4-15 SVs/CNVs detected), HIGHLY COMPLEX (>15 SVs/CNVs detected with or without the presence of chromoanagenesis).

§ ISCN 2024 formula considering CNVs >5 Mb, SVs >1 Mb, and clinically relevant SVs <1 Mb, including interchromosomal and intrachromosomal translocations. In highly complex cases (patients #18 and #24) with numerous SVs, the chromosomal formula is not specified due to their great complexity

[a,b] Results from the same patient with Kappa IgA MM (patient #21) obtained at baseline (a) and at the time of progression six months later (b).

SUPPLEMENTARY FIGURE 1

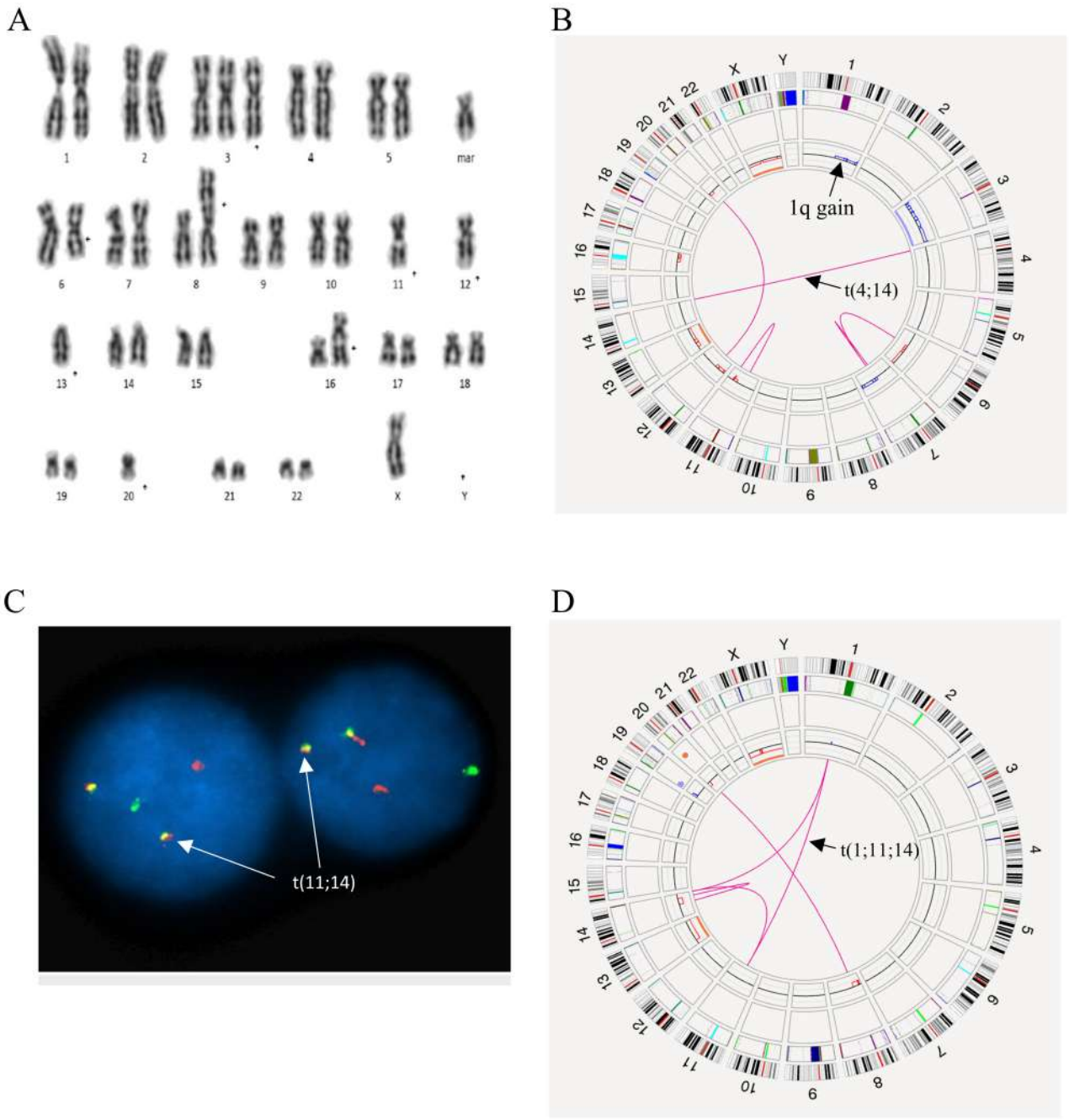

Figure 1. Chromosomal alterations identified by Optical Genome Mapping (OGM) compared to findings from conventional cytogenetic techniques. (A) Karyotype and **(B)** *Circos plot* of chromosomal alterations obtained using Bionano Access software for a patient with plasma cell leukemia (patient #23). The karyotype shows a complex hypodiploid profile (43 chromosomes), while OGM provides a more detailed and accurate representation of chromosomal abnormalities, including partial deletions in chromosomes 6, 11, 12, 16, and 20 as well as a gain on 7q and a t(12;20) translocation. Karyotyping identified two subclonal translocations (t(1;8) and t(1;17)) associated with the 1q gain, which were not detected by OGM because the breakpoints of the rearrangements involve regions of heterochromatin that are difficult to map. High-risk alteration relevant to disease prognosis, such as the t(4;14)(*FGFR3*::*IGH*) translocation was detected by OGM but not identified by karyotyping.
(C) FISH image showing the t(11;14)(*CCND1*::*IGH*) rearrangement using the XL MYEOV/IGH DF Dual Fusion probe (Metasystems) and **(D)** *Circos plot* of chromosomal alterations in patient #14 with multiple myeloma. Although FISH detects the t(11;14) translocation, OGM reveals that it is part of a more complex rearrangement involving chromosome 1, suggesting chromoplexy, a subtype of chromoanagenesis, among chromosomes 1, 11, and 14. OGM also identifies additional abnormalities, including monosomies of chromosomes X and 13, partial deletions in the long arm of chromosome 14 and in chromosomes 8 and 20, associated with a t(8;20) translocation, and a gain in the 19p region.
From the outer to the inner rings of the *Circos plot*, the following layers are displayed: (1) chromosomes and cytobands, (2) masked regions (heterochromatic, difficult to analyze), (3) structural variant (SV) region, (4) copy number variation (CNV) profile, and (5) in the center, inter- and intrachromosomal translocations represented as pink lines connecting the involved genomic loci. SVs<1 Mb were filtered out from the *Circos plot.*